Microstructure of high-strength foam concrete

A. Just, B. Middendorf*

TU Dortmund University – Germany

ARTICLE DATA

Article history:
Received 21 May 2008
Received in revised form
20 November 2008
Accepted 3 December 2008

Keywords:
Foam concrete
Porosity
Microstructure
Pore size distribution
Air voids

ABSTRACT

Foam concretes are divided into two groups: on the one hand the physically foamed concrete is mixed in fast rotating pug mill mixers by using foaming agents. This concrete cures under atmospheric conditions. On the other hand the autoclaved aerated concrete is chemically foamed by adding aluminium powder. Afterwards it is cured in a saturated steam atmosphere.

New alternatives for the application of foam concretes arise from the combination of chemical foaming and air curing in manufacturing processes. These foam concretes are new and innovative building materials with interesting properties: low mass density and high strength. Responsible for these properties are the macro-, meso- and microporosity. Macropores are created by adding aluminium powder in different volumes and with different particle size distributions. However, the microstructure of the cement matrix is affected by meso- and micropores. In addition, the matrix of the hardened cement paste can be optimized by the specific use of chemical additives for concrete.

The influence of aluminium powder and chemical additives on the properties of the microstructure of the hardened cement matrices were investigated by using petrographic microscopy as well as scanning electron microscopy.

1. Introduction

Mineral-bound foams with porous structure and low mass density have established themselves in the construction industry. These fine-grained concretes are based on German standard DIN 4164, which in the meantime is no longer valid. They have a mass density ≤2000 kg/m^3 and are classified as lightweight concretes [14]. Subject to the production processes, mineral-bound foams are called autoclaved aerated concrete or foam concrete. The characteristics of these building materials are described in [4,7–12,14].

In this paper, a methodology is presented for controlling the characteristics of air hardening, mineral-bound foams, which contribute to the expansion of the application type of these building materials. Already well-known manufacturing processes can be developed further in such a manner that the new resulting lightweight concretes receive reproducible characteristics. In this way, the requirements of the modern building task can be fulfilled, also within the field of design. For the description and evaluation of the microstructure of mineral-bound foams, light microscopy combined with digital image analysis [16], as well as scanning electron microscopy are suitable tools.

2. Technical Bases

Foam is a dispersive system made of gas and liquid and/or gas and solids, where the proportion of gaseous volume is dominant. With all genuine foams, each individual bubble represents a cavity closed in itself, with no gas-filled connections between neighbouring gas bubbles. In the foam, the gas is an intermittent or dispersive phase, while the continuous phase exists as a matrix or liquid [8].

* *Corresponding author*. Technische Universität Dortmund, Lehrstuhl Werkstoffe des Bauwesens, August-Schmidt-Str. 8, D-44227 Dortmund, Germany. Tel.: +49 231 755 4838; fax: +49 231 755 6063.
E-mail addresses: armin.just@tu-dortmund.de (A. Just), bernhard.middendorf@tu-dortmund.de (B. Middendorf).

1044-5803/$ – see front matter © 2008 Elsevier Inc. All rights reserved.
doi:10.1016/j.matchar.2008.12.011

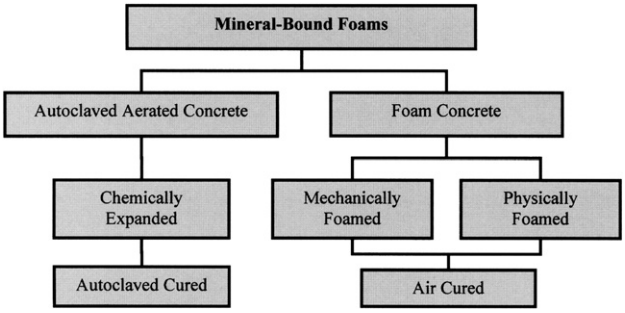

Fig. 1 – Classification of mineral-bound foams according to the manufacturing process.

Fig. 1 shows the classification of mineral-bound foams according to the manufacturing process. The process of forming air bubbles in the fresh cement paste is significant. The methods of chemical expansion, as well as physical or mechanical foaming are well known and state of the art. Autoclaved aerated concrete is based on a mortar with finely grounded, quartzitic sand, cement and/or lime and water where a foaming agent, commonly aluminium powder, is added. The stable material is cured after being removed from its mould in saturated steam atmosphere in autoclaves within a few hours and thereby receives its final properties [14,15].

Foam concretes are given their structure for foaming by using foam generators or stirring up the cement paste using foaming agents and fast rotating pug mill mixers. The paste consists of the binder, usually cement, finely grounded quartzitic sand, water and foam generating admixtures. After moulding the foam, the concrete hardens under normal atmospheric conditions.

During the mechanical foaming procedure, a foam agent is added to the mortar. Numerous bubbles are mechanically introduced by high-speed mixers. A relatively unstable foam develops with an irregular structure and undefined void structures [11]. In practice, a more usual manufacturing method is physical foaming. A pre-manufactured foam consisting of water and chemical admixture is mixed with the additional components. Under these conditions, a more stable and fine pored mortar will result [11].

Autoclaved aerated concretes are commonly used as building units, wall and ceiling panels, and as non-reinforced, as well as steel-reinforced structural elements. These construction units are used for building houses and industrial buildings. The main fields of application for foam concrete are currently backfilling and level reconciliation. Until now, the use as construction building material for load-bearing construction units cannot be achieved with the available products.

The character of the foam's porosity is significant for the physical-mechanical characteristics of mineral-bound foams. It is essential to not only put emphasis on the air voids, but also on the characteristic affecting capillary and gel porosity. Air-hardening foam concrete is strongly limited in their technical application possibilities due to its physical-mechanical characteristics. On the one hand, this is due to the high water content in the fresh mortar and, on the other hand, due to the insufficient methodology of the generating foam, which does not ensure an optimal pore distribution using today's usual procedures.

Strengths which are necessary for the use as load-bearing construction units, can currently only be achieved with the help of autoclaved hardening in a saturated steam atmosphere at temperatures of approximately 190 °C and a pressure of 1.2 N/mm^2. Among other things, the conversion of calcium hydroxide and silica to calcium-silicate-hydrate-phases (CSH) is made possible by this procedure and it also reduces the shrinking tendency of the solid.

Porosity, here essentially air porosity, in case of the aerated concrete is controlled by the additional amount and the particle size of the foaming agent aluminium. Thus, both the total air void area and a pore size distribution are adjustable. In the air void distribution, chemical foaming provides a higher regularity and higher reproducibility when compared with physical foaming.

This realization leads to the conclusion that mineral-bound, air-cured foams, which guarantee improved characteristics, should be manufactured preferably by chemical expansion. The high water content in fresh foam concretes obstructs the generation of a tight structure of the hardened cement paste matrix. To ensure a tight cement paste matrix it is necessary to decrease the water content. This leads to inconsistencies, which only can be converted to foams with the use of chemical additives.

3. Materials and Methods

The foam concretes studied were made from a cement paste without using aggregates. In part, admixtures and additives were added. In Table 1, the materials used to produce the mortar mixtures are listed.

CEM I 42.5 R according to EN 197-1 [5] was used as binder. By using different grain sizes of the aluminium powder, the air void distribution in the hardened material was controllable, whereas the air void volume was adjusted by the total quantity.

The water/cement ratio has a crucial influence on the increase of volume of the cement paste during expansion. In order to ensure an expansion in cement pastes with a low water volume, the introduction of superplasticizers based on polycarboxylatether was necessary. Furthermore, the structure of the hardened cement paste matrix was optimized

Table 1 – Basic materials used.

Binder	
Cement	CEM I 42.5 R
Additives	
Aluminium Powder	I (average ∅ 60–70 μm) II (average ∅ 20–30 μm) III (average ∅ 15–20 μm) IV(average ∅ 15 μm)
Plasticizer	PCE
Admixtures	
Microsilica	Suspension

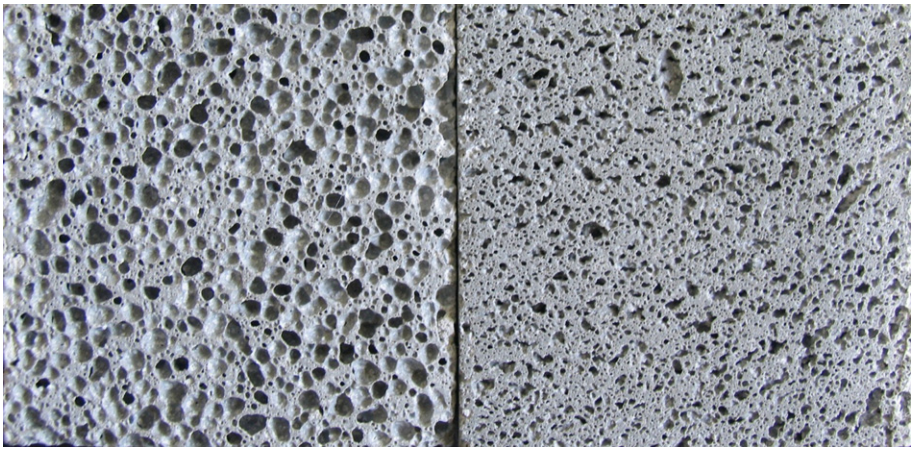

Fig. 2 – Foam concrete polished sections (left: w/c ratio = 0.45; right: w/c ratio = 0.35); total image width: 80 mm.

using the reactive additive microsilica in the form of a suspension. The samples were examined by means of light optical microscopy with an associated digital image analysis, mercury-intrusion-porosity as well as by scanning electron microscopy. The methods of investigation are described briefly in the following.

3.1. *Preparation of Polished Cross Sections*

For structural examination of foam concrete using digital image analysis, it is essential for the pores to be first saturated with coloured epoxy resin. The sample was first dried by oven drying. Removal of water from the pore channels is essential because it interferes with the penetration and polymerisation of the epoxy. The dried sample is then fitted into a mould and evacuated in a vacuum chamber. The epoxy is fed into the mould until the sample is completely submerged. After some time, the vacuum is slowly released to admit air, which pushes the epoxy into the pores. When the epoxy resin is hardened the mould was removed and the surface of the cross section was ground and polished.

3.2. *Digital Image Analysis*

The digital image analysis detects air voids by means of differences of contrast between the cement paste matrix and the air voids which are filled with coloured epoxy resin. The properties of the air voids are determined by analysing polished cross sections by means of light optical microscopy for each individual object (air void).

3.3. *Mercury Intrusion Porosity*

For the determination of the pore size distribution the mercury intrusion porosimetry were used. Therefore the sample was first dried by oven drying. After this the sample was put into a dilatometer which was afterwards filled with mercury up to a pressure of 200 Mpa. Pore radii to 4 nm could be determined.

3.4. *Scanning Electron Microscopy*

Imaging was performed in high vacuum with the application of a conductive coating. The samples were made conductive

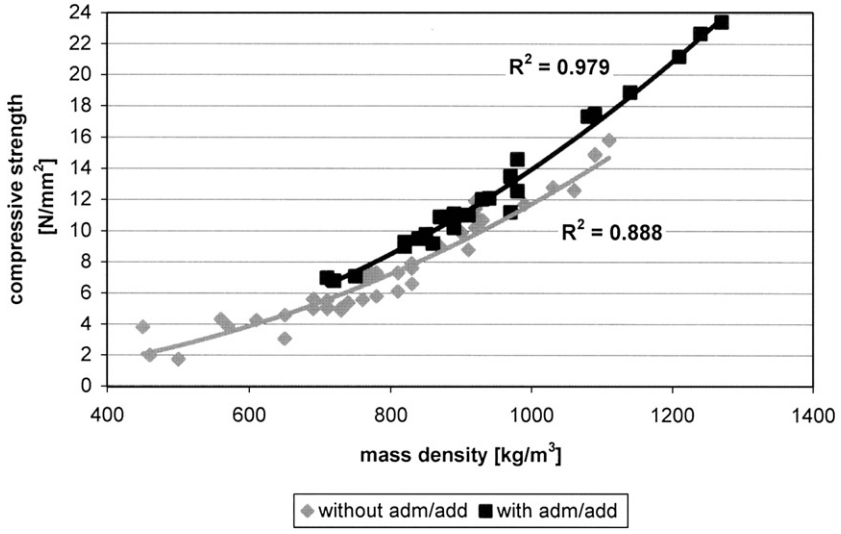

Fig. 3 – Compressive strengths as a function of the density with and without the usage on admixtures (adm) and additives (add).

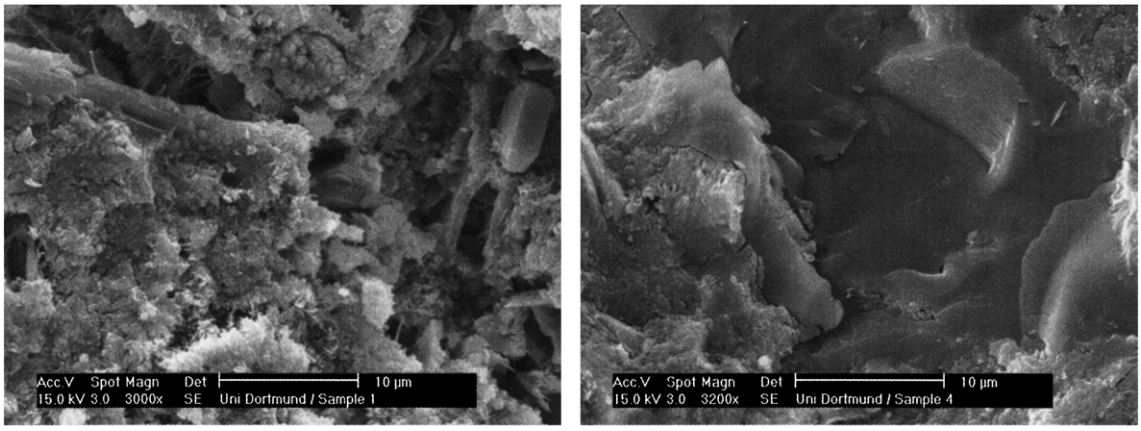

Fig. 4 – Microstructure of two foam concretes; left: w/c ratio = 0.60, without microsilica; right: w/c ratio = 0.35, microsilica content = 10%.

with a carbon and gold layer. The accelerating voltage of the scanning electron microscope was 15 kV.

4. Results and Discussion

The structure of the hardened cement paste is produced by the spatial arrangement of the matrix and the pores. The pore area is composed of the gel pores, the capillary pores, and the air voids. The existing gel porosity and capillary porosity are primarily responsible for the characteristics of the microstructure. Regarding the optimization of the structure, the same basic approaches maintain their validity for mineral-bound foams, as they were already developed e.g., in [1-3,12,13,17,18] for high performance concrete or even for ultra high performance concrete. The focus of this paper is directed towards the tailor-made structure of the air void area, as well as the structure of micropores.

The approaches of concrete technology for improving the hardened cement paste structure, like, for example, the reduction of the water/cement ratio or the use of fillers, often make the generation of an arranged air void area more difficult. For the desired sequence of the chemical reaction of expansion, a certain viscosity may not be exceeded. The consistency also affects the properties, such as mass density and strength. The lower the desired mass density is, for example, the lower the viscosity of the cement paste must be set at.

Measuring this basic consistency turns out to be particularly difficult; the chemical reaction of expansion begins

Table 2 – Compositions and strengths of the reference samples.

Specimen	Cement	w/c ratio	Microsilica [%]	Superplasticizer [%]	Compressive strength [N/mm^2]
R0	CEM I 42,5 R	0.60	0	0	48.0
R1		0.45	0	0.25	77.5
R2		0.45	5	0.75	86.8
R3		0.45	10	1.10	87.2
R4		0.40	0	0.06	67.2
R5		0.40	5	0.40	81.9
R6		0.40	10	0.73	78.3
R7		0.35	0	0.20	93.2
R8		0.35	5	0.56	102.4
R9		0.35	10	1.00	105.7

Table 3 – Compositions of the six selected sample mixtures that pore size distributions are compared in Fig. 5.

Specimen	Cement	w/c ratio	Aluminium powder [%] (No. ref. Table 1)	Microsilica [%]	Super-plasticizer [%]
E/2/0.10/0.35/0/0.20	CEM I 42,5 R	0,35	0.10 (II)	0	0.20
R7			0 (II)		0.20
E/2/0.10/0.35/5/0.75			0.10 (II)	5	0.75
R8			0 (II)		0.56
E/2/0.10/0.35/5/1.10			0.10 (II)	10	1.10
R9			0 (II)		1.00

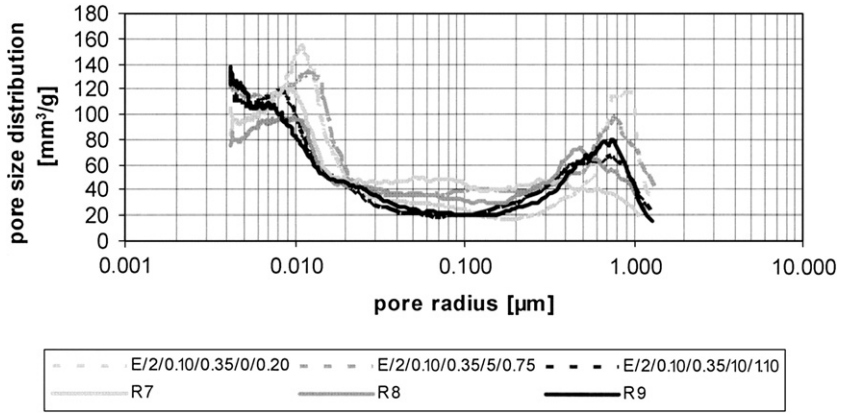

Fig. 5 – Pore size distribution of foams (E/...) and reference samples (R...)with a w/c ratio of 0.35.

during mixing and causes a constant and clear change of consistency over a small period of time. Typical measurement procedures, such as the determination of the flow time according to EN 14117 [6] or the viscosity by means of torque-controlled rheometers have proven themselves insufficient.

A characteristic of plastic mortar, which provides an explanation about the solid characteristics that can be expected, is the increase of volume during the development of foam. This reaction is finished after approximately 20 to 40 min after introducing the reaction partner, depending on temperature. Within this relatively short amount of time, this measurement provides qualitative and quantitative results that indicate the mechanical–physical characteristics of the solid material.

Fig. 2 shows the structure of two foam concretes, which differ in their composition only on the basis of the water/cement ratio. In the case of a lower water content, this leads to a stiffer fresh mortar consistency. On average, the pore size becomes smaller, the mass density and compressive strength rise.

In order to quantify the influence of the structure optimization on the compressive strength, the manufactured foam concretes are divided into two groups. The foams, which consist only of cement, water and foaming agent, are compared with the foams that were optimized additionally with chemical additives and admixtures.

Fig. 3 clearly shows the influence of the selected structure-optimizing methods by comparing overall 104 samples that differ in their compositions. The exponential trend lines, with numeric values of $R^2=0.979$ and $R^2=0.888$, agree nearly congruently with the measured individual values. The trend line of the mixtures, which were manufactured with additives and admixtures, is clearly above the trend line of the mixtures that were produced only from cement, water and aluminium.

Table 4 – Compositions of five selected sample mixtures.

Specimen	Cement	w/c ratio	Aluminium powder [%] (No. ref. Table 1)	Microsilica [%]	Super-plasticizer [%]
A/1/0.05	CEM I 42,5 R	0.60	0.05 (I)	0	0
B/2/0.10/0.40		0.40	0.10 (II)	0	0
C/3/0.08/0.40		0.40	0.08 (III)	0	0.4
D/2/0.10/10		0.60	0.10 (II)	10	0
E/2/0.10/0.45/10/0.85		0.45	0.10 (II)	10	0.85

Table 5 – Average values of the geometrical (determined by digital image analysis) and physical–mechanical properties of the five compared sample mixtures.

Specimen	Diameter [mm]	Circumference [mm]	Convex circumference [mm]	Roundness [-]	Object density [1/mm²]	Mass density [kg/m³]	Compressive strength [N/mm²]
A/1/0.05	0.323	1.311	1.129	0.716	1.591	920	11.9
B/2/0.10/0.40	0.355	1.758	1.358	0.662	1.479	930	10.7
C/3/0.08/0.40	0.402	1.861	1.491	0.641	1.432	920	10,9
D/2/0.10/10	0.299	1.395	1.161	0.698	2.149	930	12.1
E/2/0.10/0.45/10/0.85	0.290	1.264	1.094	0.708	2.795	930	12.0

Table 6 – Measuring surface, number of objects and object density of five compared sample mixtures determined by digital image analysis.

Specimen	Measuring area [mm²]	Number of objects	Object density [1/mm²]
A/1/0.05	281.1	447	1.591
B/2/0.10/0.40	267.7	396	1.479
C/3/0.08/0.40	265.4	380	1.432
D/2/0.10/10	258.3	555	2.149
E/2/0.10/0.45/10/0.85	256.9	718	2.795

The increase in the compressive strength depends on the mass density. The strength also increases with rising mass density. For a mass density of 700 kg/m³ the compressive strength increase amounts to a calculated 17% and rises for a mass density from 1100 kg/m³ to 20%.

The influence of the reduction of the w/c ratio and the simultaneous use of microsilica solidify and consolidate the microstructure of the hardened cement paste matrix. In Fig. 4 a hardened cement paste is represented on the left side, which was manufactured without additives and admixtures and with the w/c ratio of 0.60. The right side of Fig. 4 illustrates a foam concrete, which is manufactured with the w/c ratio of 0.35 and the use of superplasticizers and microsilica. A clearly more consolidated and thus firmer structure is identifiable.

The same methods for the improvement of the structure have a significantly larger influence on the properties of pure hardened cement pastes, which were manufactured without foaming agents. Comparative measurements on the reference samples R0 to R9, according to Table 2, show an increase in compressive strength with sinking water/cement ratio and rising content of microsilica. The reference samples correspond, apart from exclusion of the foaming agent, in their composition to the mixtures of the foam concretes, whose characteristics are represented in Fig. 3. The compressive strength, of 48.0 N/mm², is the lowest of all reference samples. A reduction of the water/cement ratio to 0.35 and the simultaneous addition of 10% microsilica increases the compressive strength of the reference sample R9 by 120% to 105.7 N/mm².

The strength increase in the example foam concretes is, as shown above, clearly lower.

The comparison of the microstructure of foam concretes and reference samples, whose compositions (Table 3) do not contain aluminium powder, results in comparable characteristics. The graphs of the pore size distributions in Fig. 5 show two maxima in each case for the samples examined here, which are all based on a w/c ratio of 0.35. One maximum of the pore radius ranges from 0.7 to 0.9 μm and another from 0.07 and 0.10 μm. An influence of the foaming agent on the pore sizes in the sample group evaluated here cannot be determined when compared with the reference samples. The air voids must be responsible for the slight compressive strength increasing effects on foam concretes, because the optimization of the microstructure in the hardened cement paste matrix would permit a higher strength increase.

The influence of the macro pores on the properties of the hardened foam concretes becomes clear when comparing selected samples. In Table 4, the compositions of five foams are shown.

The physical–mechanical properties of the five samples, for example, mass density and compressive strength are very similar (Table 5). The compressive strength lies between 10.7 and 12.1 N/mm² with densities of 920 and 930 kg/m³. The average values of the geometrical characteristics also specified in Table 5, however, show larger differences between the individual samples. The average values of the roundness deviate only by 12% from each other, whereas the average diameter, the average circumference and the average convex circumference differ up to 39%, 47% and 36%. The largest difference can be observed in the values of the object density (number of detected air voids). In this case, the results of the individual samples differ up to 95%.

The object density results from the quotient of the number of objects and surveyed sample area. Because the densities of the five examined specimens differ insignificantly from each other (+/−10 kg/m³), the total pore area is roughly constant in each case. Table 6 shows that the measured areas of the examples examined here are approximately constant, with sizes between 256.9 mm² and 281.1 mm². The number of

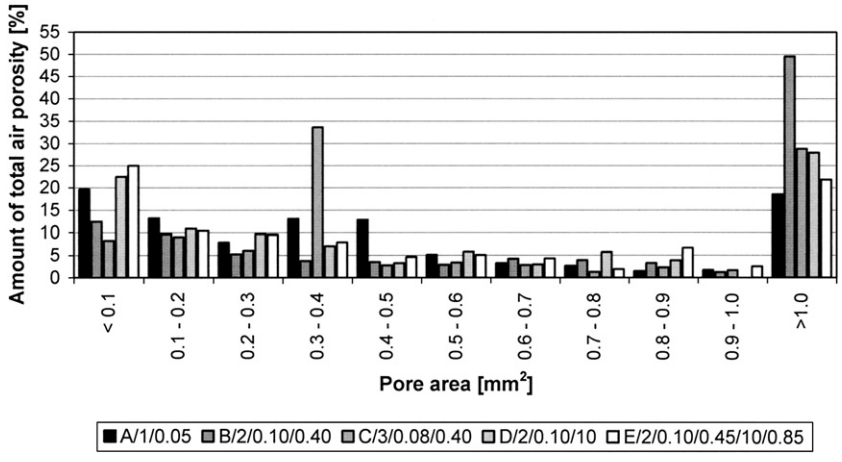

Fig. 6 – Proportion of different pore size classes of total air porosity of five compared sample mixtures.

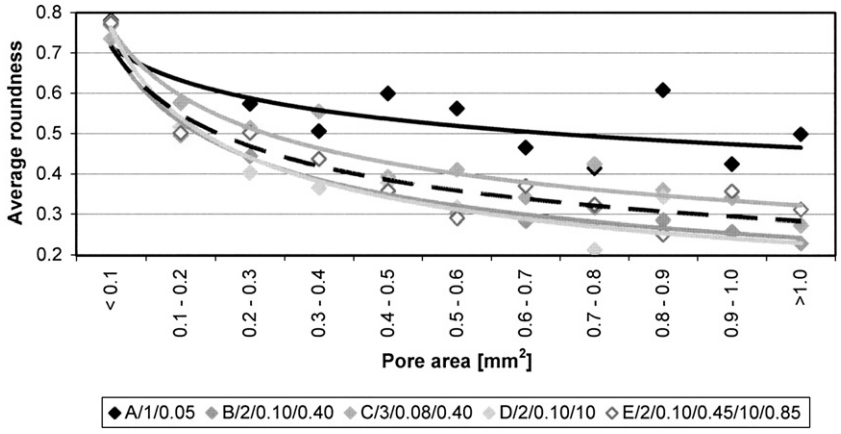

Fig. 7 – Average roundness of different air void classes of the five selected specimens.

detected air voids in this area varies between 380 and 718. This corresponds with object densities from 1.432 to 2.795 mm^{-1}.

The object density depends not only on the particle size distribution and the additional amount of aluminium powder, but also crucially on the fresh mortar characteristics. Thus, for example, the mixtures B/2/0.10/0.40, D/2/0.10/10 and E/2/0.10/0.45/10/0.85 contain 0.10% of the same aluminium powder but nevertheless the respective object densities differ by 89% with values between 1.479 mm^{-1} and 2.795 mm^{-1}.

A more detailed view of the shape of the air voids makes it necessary to arrange the objects into different classes. The area of the objects is a suitable characteristic for the classes, because this size can be determined directly on the specimen, and is not computed from another piece measured data. The diameter is also conceivable as a suitable class characteristic, but this value is computed from the measured area and therefore is subject to mathematical imperfections, such as rounding errors.

Altogether, the objects are divided into 11 classes depending on their areas. All pores with an area of less than 0.1 mm^2 and all objects with an area larger than 1.0 mm^2 form a class in each case. The areas between 0.1 mm^2 and 1.0 mm^2 are divided into nine classes with a width of 0.1 mm^2 in each case. The amount of total air porosity, not the number of objects, is crucial for the influence the air voids of the different classes have on the properties of foam concretes.

In Fig. 6, it is shown that, in most cases, the classes <0.1 mm^2 and >1.0 mm^2 possess the largest amounts of overall porosity. The sample C/3/0.08/0.40 is an exception , which exhibits the largest amount in the class between 0.3 and 0.4 mm^2. In all samples, the most part of the objects are in the class <0.10 mm^2. In this class, between 224 and 573 air voids can be detected for each measuring area. In contrast in the class >1.0 mm^2 fewer air voids are found, with 8 to 17 objects. Due to their size, these represent between 18.6% and 49.6% of the total pore surface.

The shape and pore radius distribution of the air voids are essentially responsible for the properties of the hardened foam concrete. The structural differences within the air voids become clear when observing the roundness of the pores. Fig. 7 proves that, with all examined samples, the roundness tends to decrease with rising pore sizes.

The roundness of the pores with a surface of less than 0.1 mm^2 is very similar for all samples, with values from 0.735 to 0.781 and has the least deviation from the cross section of all classes. Because these pores develop in all cases similarly, the influence on the compressive strength must take place via the pores with an area larger than 1.0 mm^2. This class represents the most significant portion of the area.

The roundness of the air voids of the class >1.0 mm^2 ranges between 0.499 for the sample A/1/0.05 to 0.230 for the sample D/2/0.10/10. These differences are justified in the consistency

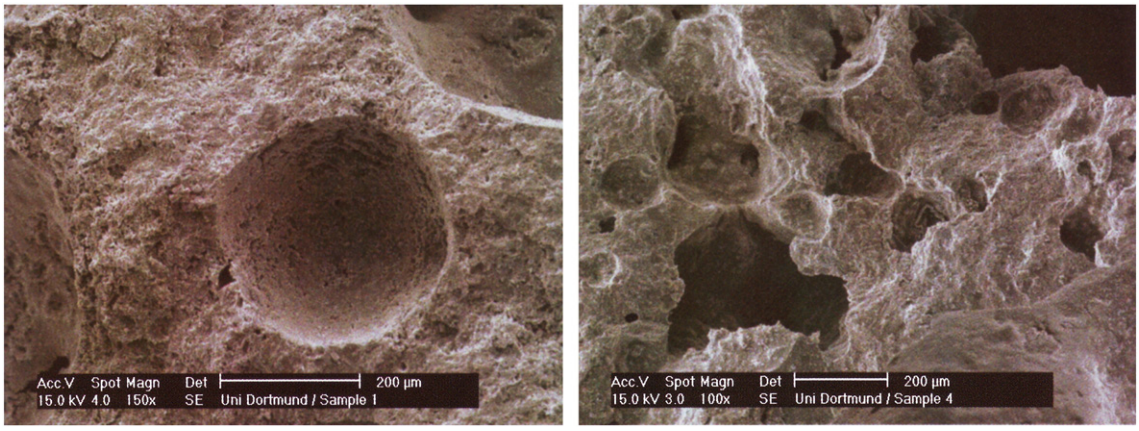

Fig. 8 – Air voids in two foam concretes: left: w/c ratio = 0.60, no microsilica; right: w/c ratio = 0.35, microsilica content = 10%.

of the fresh mortar. The high water content of the sample A/1/0.05 permits the production of a foam with the dry bulk density of 920 kg/dm^3 when using an aluminium ratio of 0.05%. The remaining samples represented here reach this dry bulk density only with an accordingly higher aluminium ratio of 0.08 and 0.10%. This means that the roundness of the air voids decreases when the generation of gas bubbles is obstructed by stiffer fresh mortar consistency.

This change to the air voids results in a reduction of the compressive strength when comparing the samples A/1/0.05 with E/2/0.10/0.45/10/0.85, because the hardened cement paste matrix solidified due to the reduced water/cement ratio and due to the use of admixtures and additives, as shown by the analysis of the reference samples.

All important results can also be derived qualitatively from Fig. 8. With decreasing w/c ratios and simultaneous use of microsilica, the average diameter of the air voids decreases and at the same time the object density increases. Furthermore, the quantity of irregularly formed pores increases considerably. The smaller the diameter of the pores, the more regularly they are formed. Regularly formed air voids increase the compressive strength with comparable densities.

5. Conclusions

It is technically possible to manufacture air-hardening, mineral-bound foams, which can be used as load-bearing structures. This foam concrete should be preferably produced using chemical foaming. Furthermore, it can be stated that mineral-bound foams, which should have increased compressive strengths, must be adjusted in such a way that they preferably possess as few air voids as possible, with a cross-section area of more than 1.0 mm^2. The generation of air voids whose cross sections deviate with increasing size from the circular cross-section is the result of more stiff fresh concrete in consistencies, as well as the use of plasticizers. Independent of the mortar recipe, air voids with a cross-section area smaller than 0.1 mm^2 are consistently formed.

REFERENCES

[1] R. Bornemann, M. Schmidt, E. Fehling, B. Middendorf, Ultra-Hochleistungsbeton UHPC — Herstellung, Eigenschaften und Anwendungsmöglichkeiten, Beton— und Stahlbetonbau 96, Nr. 7, S. 458–467, Verlag Ernst & Sohn GmbH & Co. KG, Berlin 2001.
[2] Deutscher Ausschuss für Stahlbeton, Heft 438, Hochfester Beton, Beuth Verlag GmbH, Berlin 1994.
[3] DIN 4164, Gas- und Schaumbeton — Herstellung, Verwendung und Prüfung, Richtlinien, Ausgabe 10.1951.
[4] DVGW (Deutscher Verein des Gas und Wasserfaches e.V.) — Arbeitsblatt W 307, Richtlinien für das Verfüllen des Ringraumes zwischen Druckrohr und Mantelrohr bei Wasserleitungskreuzungen mit Bahngelände, Ausgabe 10.1977.
[5] EN 197-1. Cement — Part 1: Composition, specifications and conformity criteria for common cements; 2004. German version EN 197-1:2000 + A1.
[6] EN 14117. Products and systems for the protection and repair of concrete structures — test methods — determination of time of efflux of cementitious injection products; 2004. German version EN 14117.
[7] Gundlach H. Dampfgehärtete Baustoffe. Wiesbaden: Bauverlag GmbH; 1973.
[8] S. Karl, Leichtzuschlag-Schaumbeton als Konstruktionsleichtbeton mit abgeminderter Rohdichte, Dissertation, Darmstadt 1979.
[9] R. Lewandowski, Fließfähiger Porenbeton, Bauwirtschaft, Band 32, Heft 30, Seite 1215 — 1219, Bauverlag, Gütersloh 1978.
[10] G. Nussbaum, H.-W. Vißmann, C. Grahlke, G. Drinkgern, Schriftenteihe Spezialbetone Band 2: Faserbeton, Porenleichtbeton, Dränbeton, Verlag Bau + Technik GmbH, Düsseldorf 1999.
[11] Readymix, Sonderdruck vol. 37, Fließfähiger Porenbeton, Transportbeton Beratungsgesellschaft, Ratingen 1978.
[12] de Larrard F, Sedran T. Mixture proportioning of high-performance concrete. Cement and Concrete Research 2002;32(11):1699–704.
[13] de Larrard F. Ultrafine particles for the making of very high strength concrete. Cement and Concrete Research 1989;19(2): 161–72.
[14] Verein Deutscher Zementwerke e.V., Zementtaschenbuch, 50. Ausgabe, 2002, Verlag Bau + Technik GmbH, Düsseldorf 2002.
[15] Weber H, Hullmann H. Porenbeton Handbuch; 5. Auflage, Bundesverband Porenbeton, Wiesbaden; 2002.
[16] Sánchez-Arévalo FM, Pulos G. Use of digital image correlation to determine the mechanical behaviour of materials. Materials Characterization 2008;59(11):1572–9.
[17] T. Richter, Hochfester Beton — Hochleistungsbeton, Verlag Bau + Technik GmbH, Düsseldorf 1999.
[18] Cwirzen A, Penttala V, Vornanen C. Reactive powder based concretes: Mechanical properties, durability and hybrid use with OPC. Cement and Concrete Research 2008;38(10): 1217–26.